

# Influence of the Spray Velocity on Arc-Sprayed Coating Structures

H.-D. Steffens and K. Nassenstein

(Submitted 6 September 1996; in revised form 8 September 1998)

Thermal spray processes such as plasma spraying and HVOF have gained markets due to a steady process of development of materials and equipment. One disadvantage of thermal spray processes is that costs must be competitive compared to techniques such as PTA and electroplating. In order to reduce costs, the more economical spray processes like conventional wire flame spraying, as well as arc spraying, are becoming more popular. There are modern arc spray gun designs on the market that meet the requirements of modern coating properties, for example aviation overhaul applications as well as the processing of cored wires. Nevertheless, the physical basis of arc spraying is well known. The aim of the present investigation is to show how the influence of spray velocity (not particle velocity) affects coating structure with respect to arc spray parameters.

**Keywords** arc spraying, chromium steel X46Cr13, microstructure, NiCr80 20, porosity, substrate relative velocity

## 1. Background: Arc Spray Technique

Due to the progress in technology providing electrical energy in sufficient quantity and power, Schoop developed the arc spray process in 1920 (Ref 1). Arc spraying and flame spraying are the oldest techniques. Moreover, the arc spray process has been applied in industrial use for more than 30 years and shows a wide variety of applications (Ref 2, 3). An abundance of fundamental research work has been completed about this thermal spray process (Ref 4, 5).

The arc itself is influenced by several effects and is compared to a discontinuously burning welding arc. The factors that affect an irregular arc burning and thus, cause continuous arc voltage fluctuations are the atomizing jet stream and the melting particles of the wire tips (Ref 4). The area of the arc on the wire tips is reduced as well as the diameter of the arc column due to spreading of the particles. Thus, changes of the arc between the front and the rear of the wire tip area are visible by high velocity cinematography. A superimposition of an alternating current voltage appears due to the changing conditions for arc burning. Therefore, a short arc length is preferable because any interference effects are reduced. A short arc operates more stable than a longer arc. Moreover, high melting rates are

H.-D. Steffens, Institute of Materials Technology, University of Dortmund, Germany; and K. Nassenstein, GTVmbH, Materials, Parts and Engineering for Thermal Spray Technique, Betzdorf, Germany. Contact K. Nassenstein at e-mail: gtvmbh@rz-online.de.

achieved, and there is a reduced loss of alloying elements (Ref 4).

The formation and the kinetic energy of the atomized particles on their way to the substrate are influenced by the properties of the atomizing gas jet and the metallic spray material. Mainly, the process parameter and the applied nozzle system of the arc spray gun, the atomizing gas pressure, the voltage and current, and the wire feed rate affect the spray particles and thus, the coating structure.

The spectrum of arc-sprayed particle diameters is extremely wide and measures between 2 and 200  $\mu\text{m}$  (Ref 6). A significant improvement concerning atomizing the melt of the wire tip was the design of the so-called closed nozzle system, which provides a finer atomization of the particles and a sharper focused spray jet (Ref 7). This leads to a finer coating structure that exhibits a higher oxide content (Ref 8).

High electrical energy at low wire feed rates causes higher arc temperatures and consequently high specific melting energy ( $>40$  kJ/kg). Due to a lower viscosity of the melting material, finer particles are formed with a higher oxide content in the coating structure. Moreover, a loss of alloying elements (carbon, chromium) can be observed when spraying steel, and this results in a poor coating structure (Ref 4, 6).

**Table 1** Variation of arc spray parameters

Parameter	Variation
Surface velocity ( $v$ ), m/min	5, 35, 70, 100
Voltage ( $U$ ), V	25, 30, 35
Current ( $I$ ), A	200, 300
Atomizing gas pressure ( $p$ ), bar	3, 4, 5
Atomizing gas system	Open, closed

**Table 2** Chemical composition of the applied thermal spray wire

Material	Chemical composition, wt%							
	Ni	Cr	Cu	C	Fe	Mn	Si	S
X46Cr13	...	12.5-14.5	...	0.42-0.5	bal	1.0	1.0	0.03
NiCr8020	76 min	18-21	0.5	0.25	0.5	1.2	0.5	0.015

Nevertheless, arc spraying is a most efficient coating process with regard to the exploitation of energy for melting the material via the thermal spray technique (Ref 9). Arc spraying is a well-known and investigated process. However, one factor that has not been investigated sufficiently (Ref 10) is the question on how the spray velocity affects the coating structure.

## 2. Experimental Procedures

An arc spray gun type LD/U2 (OSU, Germany) was connected to the power supply type Metalliser V300 (Metallisation, Great Britain) with a maximum current output of 300 A (Fig. 1). The specimen rotated during deposition at different rotation velocities. Also spray parameters, such as voltage, current, and atomizing air pressure, were varied (Table 1). The spray distance was measured as 150 mm. Two different metal materials were applied: (a) 13% chromium steel wire, 1.6 mm diameter according to German Standard DIN 8566, and (b) 80Ni-20Cr wire, 1.6 mm diameter, according to German Standard DIN 8566 (Table 2).

The spray velocity was increased by increasing the rotation of the lathe chuck. The transverse velocity of the support was kept constant at 1 m/min. Pipe segments with a diameter of 90 mm and a wall thickness of 3.2 mm were used as the substrate material.

## 3. Results and Discussion

### 3.1 Steel Coatings

Figures 2 to 4 show the structure of X46Cr13 coating obtained at different spray velocities. The structure obtained for arc spraying is the typical lamellae character. The coating structure prepared at a velocity ( $v$ ) of 5 and 35 m/min is more dense compared to the coating prepared at 100 m/min. The higher velocity coating exhibits more pores, which are lenticular in shape. Moreover, the layers appear to have poor cohesion. This effect is supported by sickle-shaped inhomogeneities in bonding (Fig. 4b).

Basically, two main physical parameters influenced the porosity: particle velocity and temperature. Increasing the particle

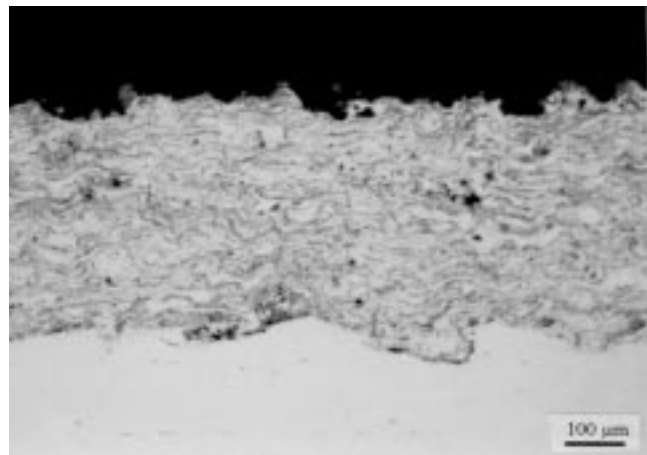
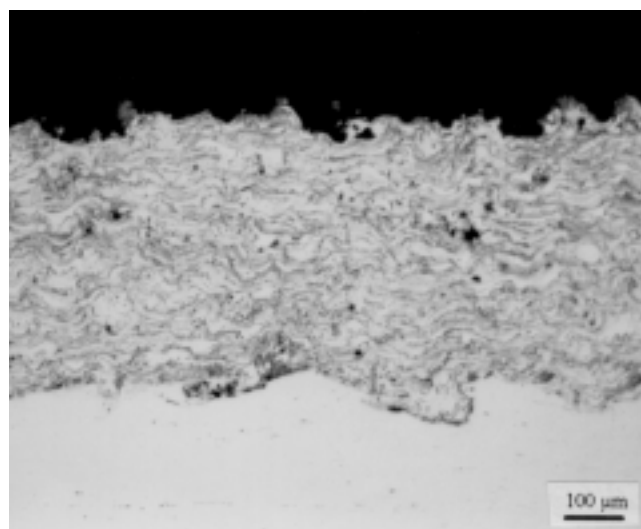


**Fig. 1** Setup for coating the pipe segments

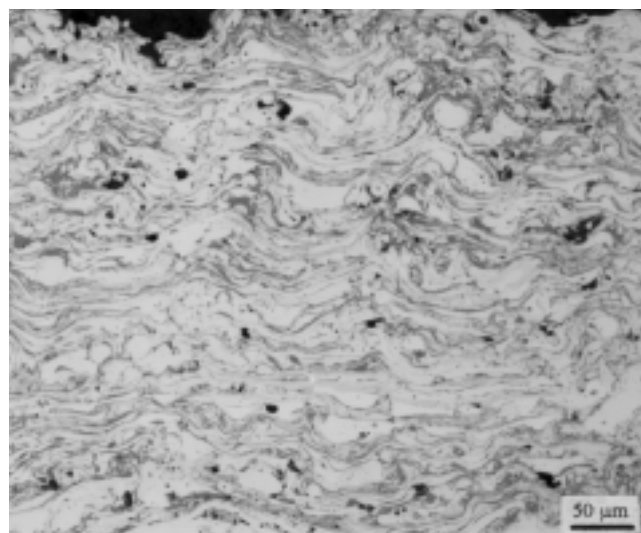
temperature decreases the viscosity of the impacting particles. Thus, the coating roughness is reduced. The closed nozzle system supports a finer atomization of the melt by a radial jet stream focused on the arc. Consequently smaller, hotter, and faster spray particles are produced, which form a denser structure (Fig. 5). At the same time a higher oxide content can be observed. Light microscopy reveals a darker color structure due to weaker contrast of the oxides. Additionally, there are solidified particles in all coatings.

The quantity and size of the solidified particles relates to the rotation velocity but depends on the primary spray parameters (compare Fig. 2a with Fig. 6). The coatings  $v = 5$  m/min and  $v = 35$  m/min show excellent bonding to the substrate. While only a few pores can be noticed in the interface, the 100 m/min coating shows a higher quantity of pores.

The results of the image analysis system support the visual differences in the arc-sprayed structure. While the minimum diameter ( $D_{\min}$ ) of pores stay constant, the maximum diameter

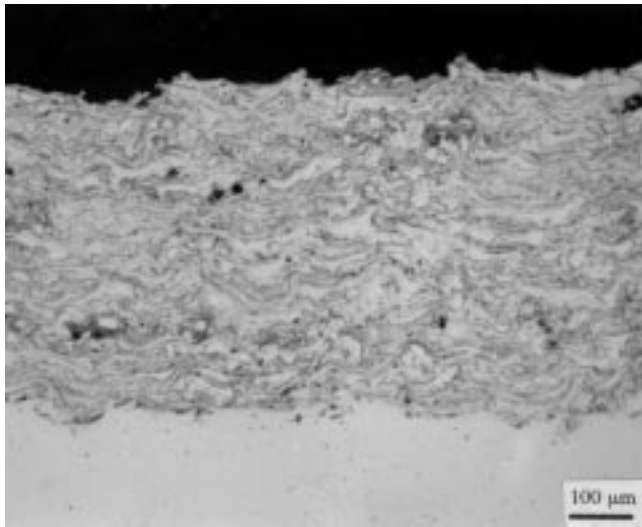


(a)

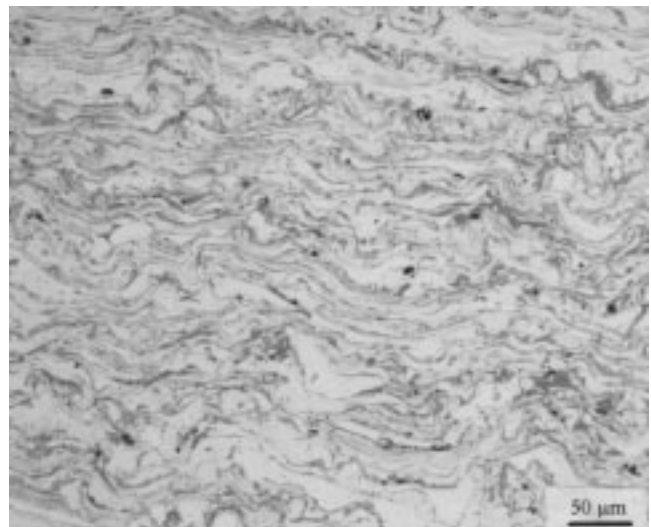


(b)

**Fig. 2** Cross section of a X46Cr13 coating sprayed with closed nozzle system.  $p = 4.5$  bar,  $I = 200$  A,  $U = 25$  V,  $v = 5$  m/min

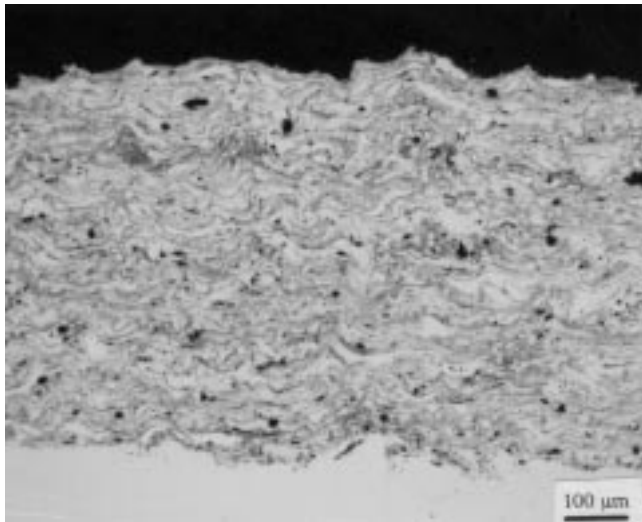


(a)

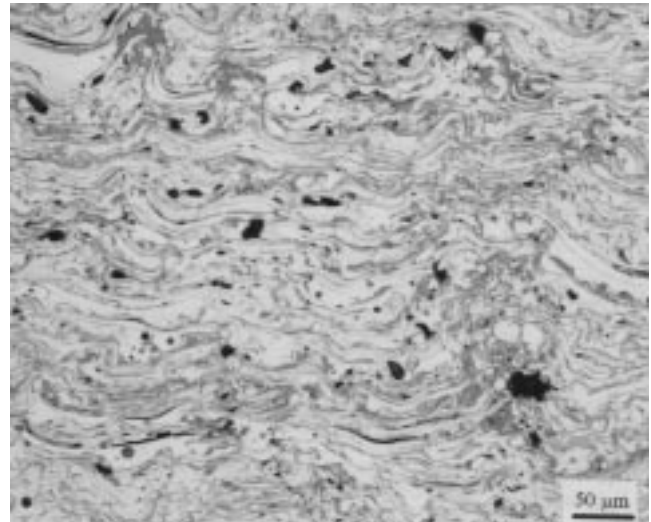


(b)

**Fig. 3** Cross section of a X46Cr13 coating sprayed with closed nozzle system.  $p = 4.5$  bar,  $I = 200$  A,  $U = 25$  V,  $v = 35$  m/min



(a)



(b)

**Fig. 4** Cross section of a X46Cr13 coating sprayed with closed nozzle system.  $p = 4.5$  bar,  $I = 200$  A,  $U = 25$  V,  $v = 100$  m/min

( $D_{\max}$ ) increases with increasing rotating velocity (Fig. 7). This fact indicates an oval shape of the pores at higher velocities.

Increasing the atomizing air pressure causes the same effect as the closed nozzle system. Higher atomizing pressure results in the previously described coating structure (Fig. 8).

Low wire feed rates and consequently low spray currents at constant voltage result in a higher specific energy for arc melting the wire. The reason for this effect is based on a factor of proportionality between wire feed rate and current that is smaller than one for the arc spray system; for example, doubling the wire feed rate increases the current by less than twice its value. However, the influence concerning the porosity is not as strong compared to the increase of atomizing gas pressure or applying a closed nozzle system instead of an open system. Nevertheless, the average values of porosity indicate a general tendency (Fig. 9).

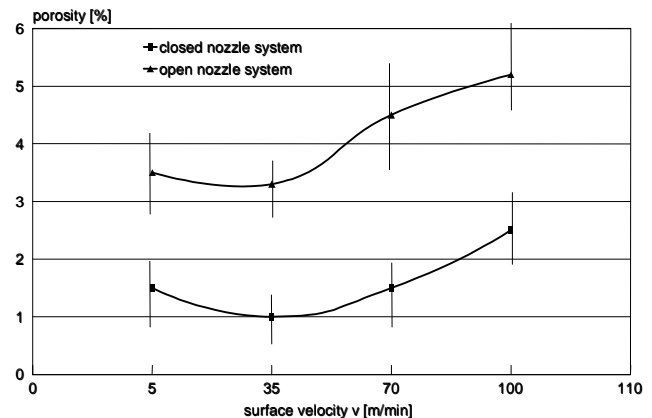


**Fig. 5** Porosity depending on surface velocity and choice of nozzle system, X46Cr13.  $p = 4.5$  bar,  $I = 200$  A,  $U = 25$  V

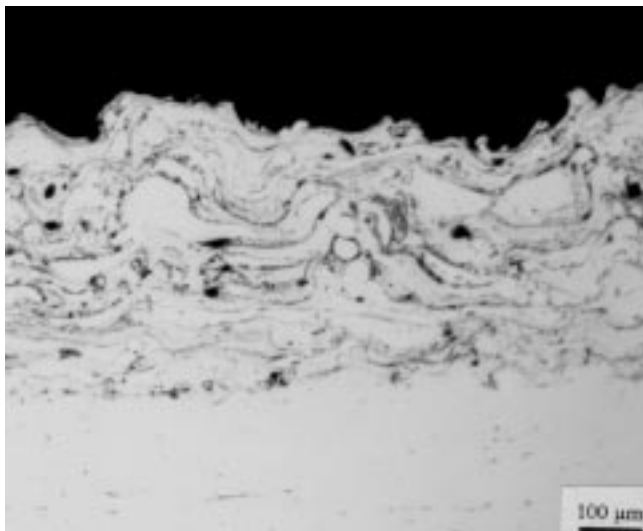


**Fig. 6** Cross section of a X46Cr13 coating sprayed with an open nozzle system.  $p = 4.5$  bar,  $I = 200$  A,  $U = 25$  V,  $v = 5$  m/min

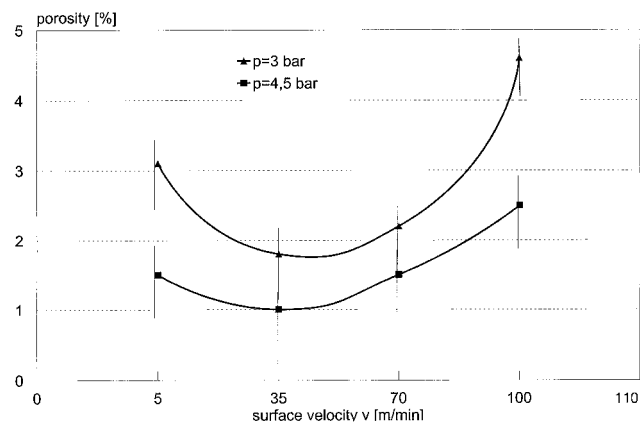


**Fig. 8** Porosity depending on surface velocity and atomizing gas pressure, X46Cr13, sprayed with closed nozzle system.  $I = 200$  A,  $U = 25$  V

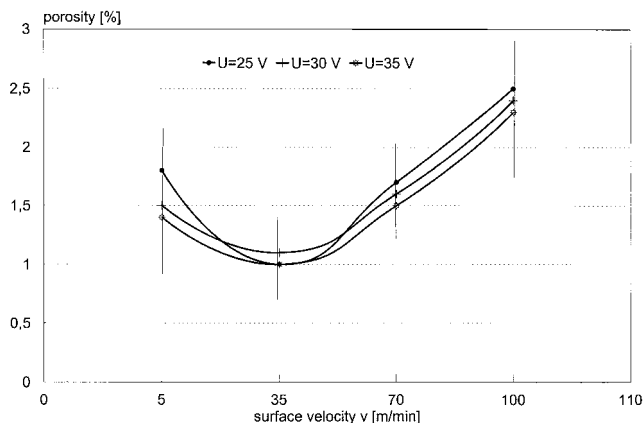


**Fig. 10** Porosity depending on surface velocity and output voltage, X46Cr13, sprayed with closed nozzle system.  $p = 4.5$  bar,  $I = 200$  A

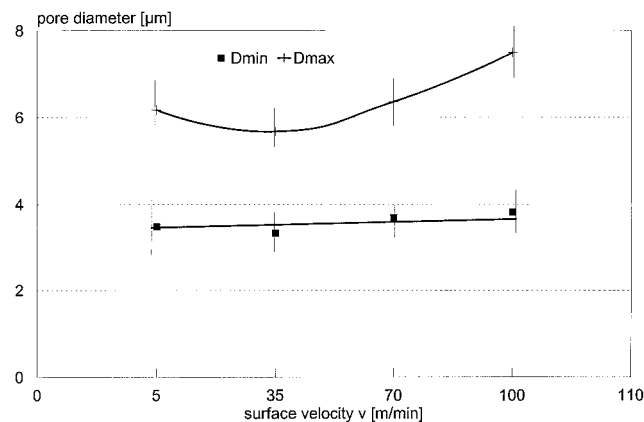


**Fig. 7** Maximum and minimum pore diameter depending on surface velocity, X46Cr13, sprayed with closed nozzle system.  $p = 4.5$  bar,  $U = 25$  V,  $I = 200$  A

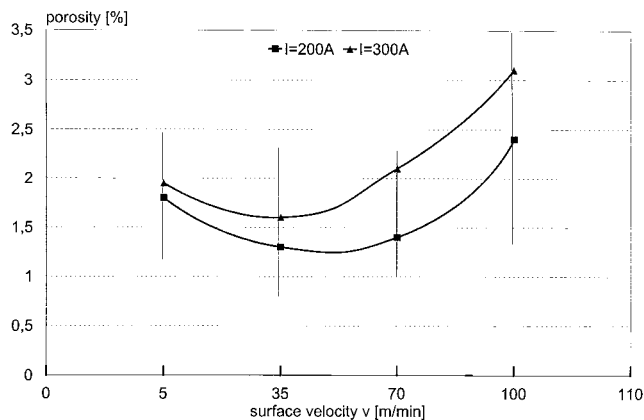


**Fig. 9** Porosity depending on surface velocity and current, X46Cr13, sprayed with closed nozzle system.  $p = 4.5$  bar,  $U = 25$  V

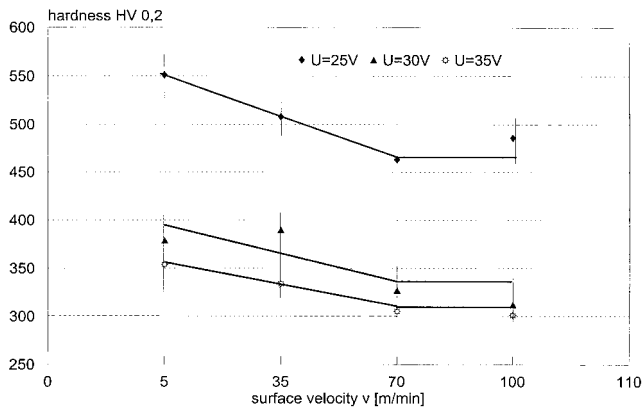
Varying the output voltage for the arc had no significant influence on the porosity (Fig. 10). This effect was based on the arc voltage itself, which was superimposed by an alternating current (ac) voltage forced by the motion of the arc between the wire tips (Ref 4). The effective applied voltage of the arc and consequently the melting power varies in the range of  $\pm 10$  V. There is no constant value for the effective melting power that is applied to a single melting particle. Nevertheless, higher output voltages provide a hotter melt and form fine particles, which result in a denser structure with a higher amount of oxides.

Figure 11 infers a higher loss of alloying elements (chromium and carbon) at higher voltages, which lead to a lower hardness. Moreover, an increased porosity produces a lower hardness with increasing rotating velocity.

Next, a model is used to explain the increase of the porosity with increasing rotating velocity. First considerations led to the assumption that physical forces are responsible. Impact and centrifugal force of an impacting particle are assumed to interact. The porosity might increase because of higher centrifugal force due to higher rotation speed. But a simple calculation indicates that the impact forces are greater than the centrifu-

gal force by a factor of  $8.1 \times 10^5$ , assuming a solidifying time on impact of  $10^{-6}$  s. This fact excludes the influence of these forces (Fig. 12).

Figure 13 shows a sketch of coating buildup from single layers applied at different rotating speeds. Increasing the rotating speed of the specimen (and thus the surface velocity) decreases the dwell time of the impacting particle on the substrate. Less particles impact per rotation on the surface because of the relatively short time. In the given model a  $500 \mu\text{m}$  coating can be formed by applying two layers at 5 rpm. The same coating thick-



**Fig. 11** Hardness depending on surface velocity and output voltage, X46Cr13, sprayed with closed nozzle system.  $p = 4.5 \text{ bar}$ ,  $I = 200 \text{ A}$

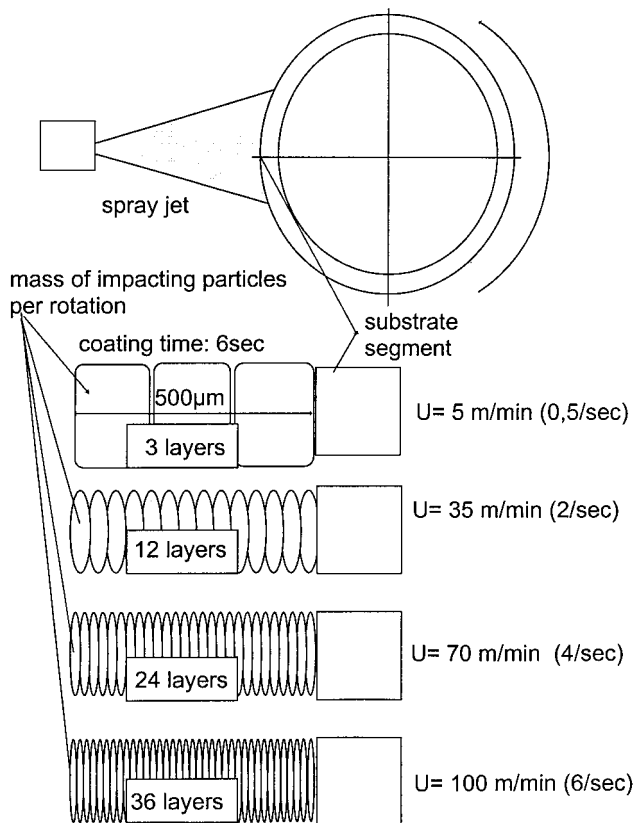


**Fig. 13** Model for formation of coating applying different surface velocities

ness is produced at 35 rpm with 12 layers, 70 rpm with 24 layers, and 100 rpm with 36 layers. The coating time is constant in all cases. During the formation of the coating a self-densifying process is initiated because impacting particles shot peen the surface. Thus, the roughness is reduced, and pores are mostly avoided. Lower velocities support this effect because of the greater mass of impacting particles. The cross sections confirm this thesis because the last layer exhibits more pores than the underlying layers, even for a coating produced at low surface velocities.

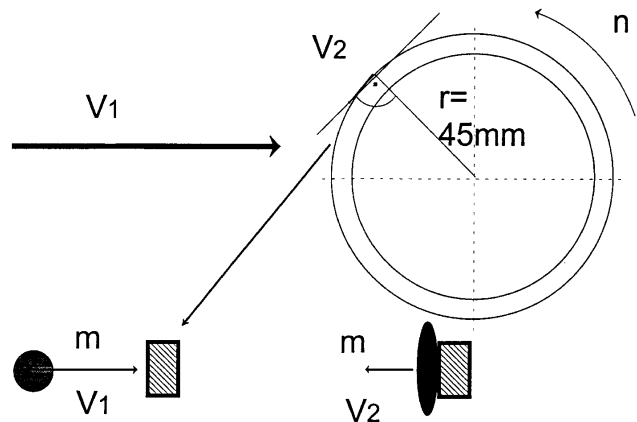


**Fig. 12** Approximate calculation of forces applied on spray particles

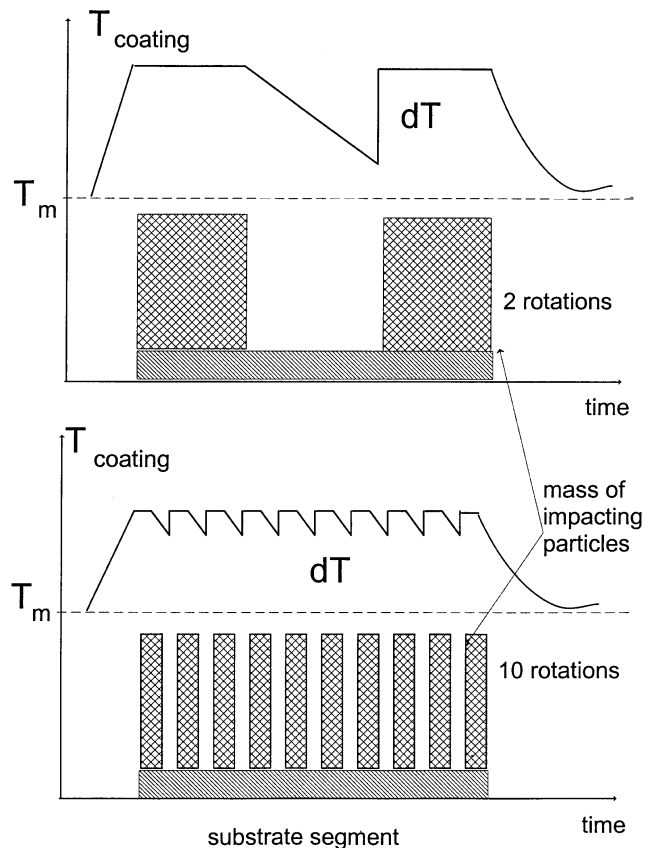


**Fig. 14** Model for coating temperature at different surface velocities

On the other hand, contraction processes and outgassing resulting from the temperature gradient during arc spraying influence the porosity. A higher temperature gradient results in greater outgassing and shrinkage forces in each layer. Both are initiated by fast resolidifying steel materials forming pores in the structure. The gas content of the steel cannot be contained within the metal lattice (Ref 4). The heat input during the production of a certain coating mass does not change its total amount while increasing the surface velocity. However, the peaks of the average coating temperature  $T_m$  of a coating decrease because of less impacting particles. A reduced porosity is obtained (Fig. 14) due to the lower temperature gradient and consequently smaller shrinking forces.

Two effects are superimposed on each other with increasing surface velocity, that is, (a) a reduced self-densifying effect of the sequentially impacting particles and (b) a reduced temperature gradient, which leads to lower outgassing, as well as to lower shrinkage forces. This model explains the porosity

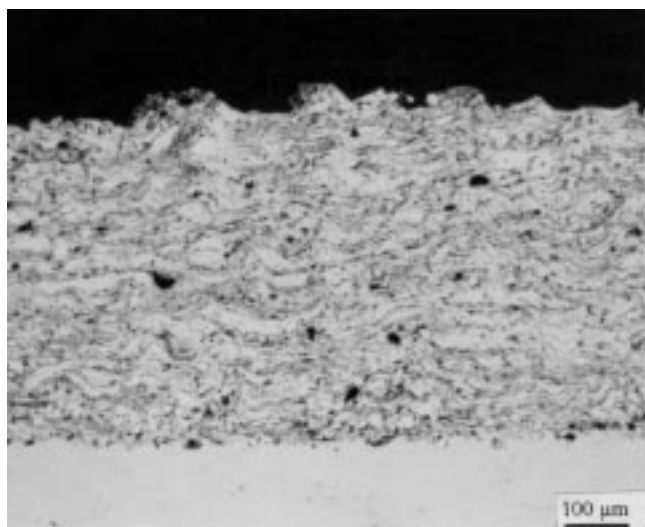


**Fig. 15** Cross section of a 80Ni20Cr coating.  $p = 4.5$  bar,  $I = 200$  A,  $U = 25$  V,  $v = 5$  m/min

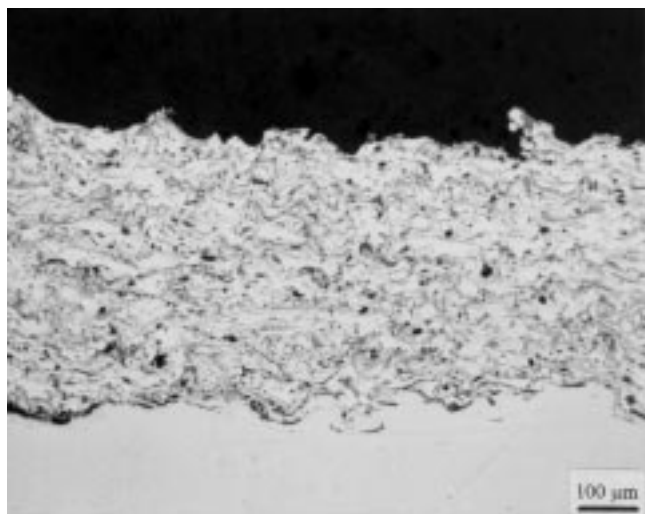


**Fig. 17** Cross section of a 80Ni20Cr coating.  $p = 4.5$  bar,  $I = 200$  A,  $U = 25$  V,  $v = 100$  m/min

minimum in the range of 35 m/min ( $\sim 0.6$  m/s), which is supposed to be an optimized surface velocity for arc-sprayed mild steel coatings (compare Fig. 3 and 8). In this range an optimum of temperature influence and self-densifying effect is obtained.

### 3.2 80Ni-20Cr Material

Similar to the steel structures, a qualitative increase of the coating porosity with increasing surface velocity was noticed while the cross sections were investigated (Fig. 15 to 17). However, a more homogeneous structure with a lower oxide content was formed.

Results of the image analysis confirm the qualitative observation (Fig. 18). Increasing the atomizing gas pressure influenced the porosity more significantly compared to the mild steel coatings. This effect was based on the higher density of 80Ni-20Cr ( $\rho = 8.68$  kg/m<sup>3</sup>) compared to steel ( $\rho = 7.8$  kg/m<sup>3</sup>). The melting particles were slightly accelerated and reached lower particle velocities. Basically, NiCr coatings were more porous

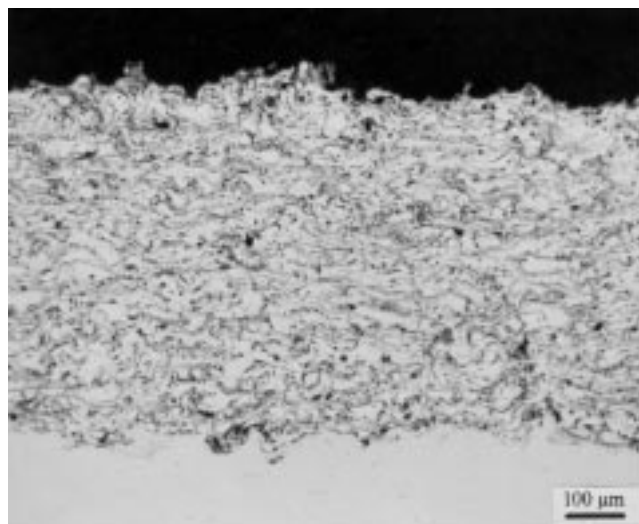


**Fig. 16** Cross section of a 80Ni20Cr coating.  $p = 4.5$  bar,  $I = 200$  A,  $U = 25$  V,  $v = 35$  m/min

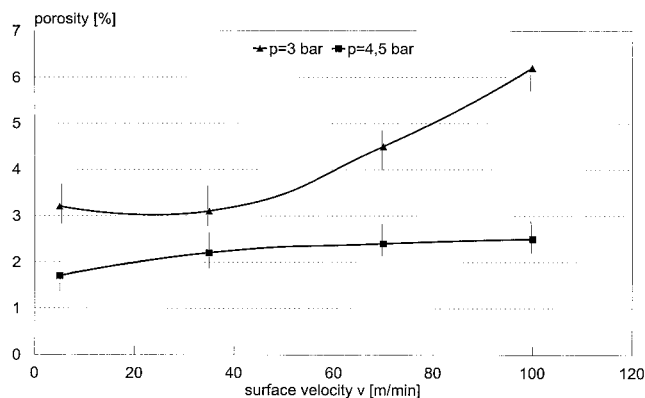


**Fig. 18** Porosity depending on surface velocity and atomizing gas pressure, 80Ni20Cr, sprayed with closed nozzle system.  $U = 30$  V,  $I = 200$  A

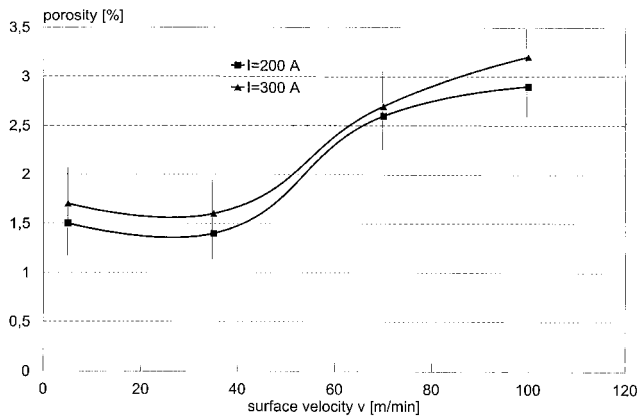


**Fig. 19** Porosity depending on surface velocity and current, 80Ni20Cr, sprayed with closed nozzle system. Atomizing gas pressure,  $p = 4.5$  bar,  $U = 30$  V

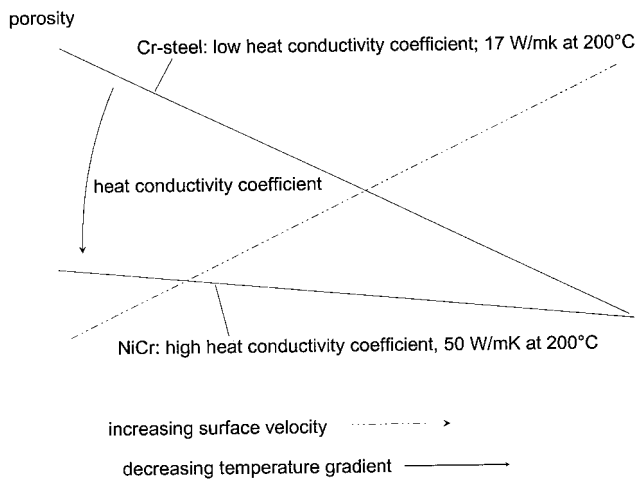


**Fig. 20** Simple draft of the influences of different heat conductivity and surface velocity on porosity of arc sprayed metal coatings

than steel when produced at higher surface velocities (compare with Fig. 8).

Figure 19 shows the porosity dependence with respect to the surface velocity and current. The increase of the porosity with increasing velocity is visible. But the minimum of the porosity in the range of 35 m/min is less significant.

The heat conductance coefficient of NiCr compared to steel (an approximate factor of 5) needs to be considered. Figure 20 shows schematically the effect of lowering the heat conductivity on the porosity. The results lead to the thesis that low surface velocities form an increased temperature gradient and, thus, a high amount of gas as well as high shrinkage forces, and consequently, high porosity arises. The heat conductivity coefficient of the coating material is responsible for transferring the heat into the cooler substrate, and a higher coefficient benefits a better heat transfer. Less pores were formed because of lower outgassing and shrinkage forces. The lower porosity of NiCr compared to steel coatings at low surface velocities confirms this fact. (Compare Fig. 9 with Fig. 19,  $v =$

5 m/min.) As a consequence, no minimum of porosity was formed.

## 4. Conclusions

In this investigation, the influence of spray velocity on the coating structure for arc-sprayed coatings was studied. Therefore, rotating pipe segments were coated with chromium steel and nickel-base alloy at different speeds. The surface velocity mainly influences the coating porosity. It is supposed that increasing surface velocity reduces the self-densifying process of the impacting particles. On the other hand, higher outgassing of the resolidifying metal as well as higher shrinkage forces are obtained at low surface velocity. Chromium steel requires a surface velocity in the range between 35 to 40 m/min for optimum porosity because of a low heat conductivity coefficient. Slow surface velocities (5 m/min) provide dense NiCr coatings because of a higher heat conductivity coefficient.

## Acknowledgment

This research was financed by the German government via Deutsche Forschungsgemeinschaft (German institution for financing basic research work).

## References

1. M.U. Schoop, *Handbook of Metal Spray Technology*, Rascher & Cie. AG Verlag, Zürich, Switzerland, 1935
2. D.R. Marantz, State of the Arc Spray Technology, *Thermal Spray Research and Applications*, T.F. Bernecki, Ed., ASM International, 1992, p 113-118
3. I. Hammad, Robotic Arc Spraying, *Thermal Spray Research and Applications*, T.F. Bernecki, Ed., ASM International, 1992, p 651-653
4. H.-D. Steffens, "Bonding and Coating Structure in Arc and Flame Spraying," Ph.D. dissertation, Hannover, Germany, 1963
5. H.-D. Steffens, "Metallurgical Action during Spraying of Steel Materials in Atmosphere and under Shrouded Gas," thesis, Hannover, Germany, 1967
6. K.H. Busse, "The Behavior of Spray Particles during Atmospheric Arc Spraying," Ph.D. dissertation, Dortmund, Germany, 1989
7. H. Schmidt and D. Matthäus, Stage of Development of the Arc Metal Spraying Systems New Experiences and Data, *Proceedings of the 9th International Thermal Spray Conference* (The Netherlands), 1980, p 225-231
8. J. Brennek and W. Milewski, The Effect of So Called Closed Atomising Chamber on the Structure and Quality of Sprayed Coatings, *Proceedings of the 9th International Thermal Spraying Conference* (The Netherlands), 1980, p 239-243
9. L.J. Grant, How Recent Advances in Arc Spraying Broaden the Range of Applications, Paper III, *12th International Conference on Thermal Spraying*, Welding Institute, 1989, p 1-17
10. U. Fischer, Contribution to the Investigation of the Influence of Dominating Process Parameters on the Properties of Plasma Sprayed Thermal Barrier Coatings, VDI Reports, Volume 5, No. 171, Germany, 1989